<연구논문>

Femtosecond Laser Ablation of Polymer Thin Films for Nanometer Precision Surface Patterning

Indong Jun[a], Jee-Wook Lee[b], Myoung-Ryul Ok[a], Yu-Chan Kim[a], Hojeong Jeon[a,*]

[a] Center for Biomaterials, Biomedical Research Institute, Korea Institute of Science and Technology, Seoul 02792, Korea
[b] School of Advanced Materials Engineering, Kookmin University, Seoul 02707, Korea

Abstract

Femtosecond laser ablation of ultrathin polymer films on quartz glass using laser pulses of 100 fs and centered at λ=400 nm wavelength has been investigated for nanometer precision thin film patterning. Single-shot ablation craters on films of various thicknesses have been examined by atomic force microscopy, and beam spot diameters and ablation threshold fluences have been determined by square diameter-regression technique. The ablation thresholds of polymer film are about 1.5 times smaller than that of quartz substrate, which results in patterning crater arrays without damaging the substrate. In particular, at a $1/e^2$ laser spot diameter of 0.86 μm, the smallest craters of 150-nm diameter are fabricated on 15-nm thick film. The ablation thresholds are not influenced by the film thickness, but diameters of the ablated crater are bigger on thicker films than on thinner films. The ablation efficiency is also influenced by the laser beam spot size, following a $w_{0q}^{-0.45}$ dependence.

Keywords : Femtosecond laser ablation, Patterned chemical surface, Polymer, Poly(ethylene glycol), Thin film

1. Introduction

Patterned surfaces have great importance for various applications, such as biological, sensor, energy, and electronic researches. Multiphoton photolithography via femtosecond laser ablation process became useful to fabricate the chemically patterned platforms due to its advantage of high-resolution material processing without photomasks and chemical developers [1,2]. Pulse duration of the femtosecond laser in this study is ~ 100 fs, resulting in extremely high peak intensity of a focused pulse and nonlinear multiphoton absorption in transparent dielectric materials [3]. There is no heat exchange during femtosecond laser pulse irradiation, which results in minimizing thermal stress and collateral damage, while thermal damage cannot be neglected from material processing with nanosecond or longer laser pulses. Therefore, the femtosecond laser induced ablation process is stable and reproducible [4,5]. The nonlinear optical characteristics of Gaussian beam profile of the femtosecond laser lead more precise ablation features smaller than the spot size of the laser pulse by adjusting the pulse energy close to the ablation threshold [6,7]. Consequently, dielectric materials which are transparent to the infrared light such as glass and polymers interact with laser pulses nonlinearly and can be ablated in subwavelength resolution using IR femtosecond laser pulses [1,6,8].

The mechanism of interaction between photons and polymers has been studied, and several models have been proposed: photochemical [9, 10], photothermal [10-12], photophysical [13] and their combination . When considering the ablation mechanisms, it should be noted that the type of polymer and irradiation light source are important. The polymer synthesis routes (radical polymerization and condensation) are

*Corresponding Author: Hojeong Jeon
Center for Biomaterials, Biomedical Research Institute, Korea Institute of Science and Technology
Tel: +82-2-958-5140 ; Fax: +82-2-958- 5308
E-mail: jeonhj@kist.re.kr

related with respective laser-induced polymer reactions (depolymerization or decomposition) [10]. Polymers that are formed by radical polymerization are depolymerized while polymers that are formed by condensation are decomposed upon irradiation [10]. The ablation mechanisms are influenced by the photon energy and pulse duration of the irradiation source [14]. In particular, ultra-short pulse-induced ablation becomes more complex due to its nonlinear optical characteristics.

The present work reports on the nanopatterning of thin films (10 ~ 70 nm) of poly (ethylene glycol) (PEG) using tightly focused single femtosecond laser pulses at 400 nm wavelength. Most previous reports on polymer ablation dealt mainly with thicker films and larger beam spot diameters [12,15-17]. PEG was chosen in the present study because it is a widely used biomaterial that can be treated by photolithography methods [18-21]. We fabricated ablated craters smaller than the diffraction limit and investigated the influence of film thickness and irradiation beam spot size. Topographies of the ablated features were obtained by atomic force microscopy (AFM) and crater diameters were measured and utilized to calculate ablation thresholds.

2. Experiments

2.1 PEG brush layer synthesis

Figure 1 shows the schematic of PEG brush layers and chemical compositions. Surface initiated atom transfer radical polymerization (SI-ATRP) was used to generate the PEG brush layer that has been shown to eliminate non-specific protein adsorption, and offers a number of advantageous properties for biotechnological applications [18,22]. The PEG brush layers were synthesized by reacting a surface grafted with the SI-ATRP silane with solution containing PEG monomethacrylate monomer (PolySciences) in a deoxygenated environment. The SI-ATRP synthesis was carried out as described previously [22]. Briefly, 1.0 mmol copper (I) bromide, 2.0 mmol bipyridine, 0.3 mmol copper (II) bromide, and 25 mmol of the monomer poly(ethylene glycol) monomethyacrylate (side chain MW = 200) were dissolved in 12 mL of methanol and 3mL of degassed water. The dark red solution was bubbled with nitrogen for 30 minutes and sonicated until all materials were dissolved, before being poured over the silanated samples. The reaction was maintained for various times to yield the desired thicknesses, under nitrogen flow before
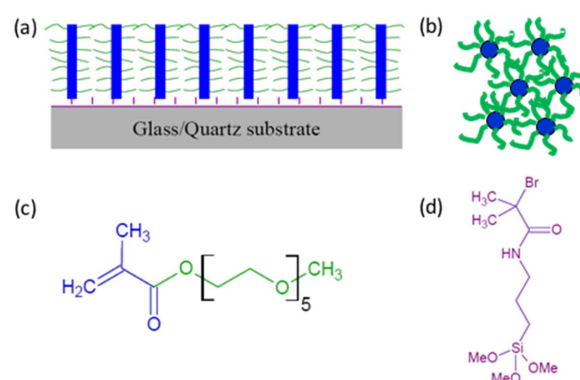

Fig. 1. Schematic of poly(ethylene glycol) brush layers on quartz glass. (a) Side view to illustrate PEG film on quartz, (b) top view of the film, (c-d) chemical structure of the polymer. Purple = synthesized silane, Blue = methacrylate backbone, Green = PEG "arms"

the samples were removed, rinsed copiously with methanol and dried under a nitrogen stream.

2.2 Laser ablation and measurement

Ablation experiments were performed in ambient air with an amplified Ti:Al$_2$O$_3$ femtosecond laser (Spitfire, Spectra Physics Inc.) of about 100 fs pulse length [at full width half maximum (FWHM)] and wavelength of ~ 400 nm that was obtained after being frequency-doubled from fundamental ~ 800 nm wavelength laser beam by a nonlinear crystal. The fluence was adjusted with an attenuator including a half wave plate (l/2) and a polarizing beam splitter (PBS). As the laser pulse energy required to ablate high- resolution features was extremely low, a neutral density (ND) filter was inserted into the beam path. To generate user-designed patterns, samples were loaded on a precise three-dimensional motorized stage with a synchronized laser firing system controlled by a programmable PC. The sample was precisely aligned perpendicular to the incident laser beam by adjusting the tilting angle of the sample. To investigate the influence of beam spot size and film thickness, long working distance objective lenses with three different numerical aperture sizes were used: 10x Mitutoyo M Plan Apo (N.A.= 0.28), 50x Mitutoyo M Plan Apo (N.A.= 0.55) and 100x Nikon CFI 60 LU Plan Epi ELWD Infinity-Corrected (N.A.= 0.8). The pulse energy was measured by a pyroelectric energy meter (Molectron J5-09) placed between the attenuator and the ND filter. Before the ablation experiments, the output energy from each objective lens and energy at the above-mentioned position were measured separately to yield the

attenuation ratios. These attenuation ratios were utilized to obtain the pulse energies in the course of the nanoablation experiment that were too low to measure via the energy meter. Using the computer-controlled system, single pulse ablation with quartz only and PEG films of various thicknesses on quartz was performed. The ablation craters were examined by AFM (Nanoscope IIIa, Veeco) with high aspect ratio tips (Nanosensors, AR5-NCHR, Aspect ratio ≥ 5:1).

3. Results and Discussion

Subwavelength-sized ablated features on polymer thin films were fabricated by single laser pulses at various energies using a 100x objective (Fig. 2). For pulse energies of 4 and 4.5 nJ, the PEG film was ablated from the quartz substrate with no damage to

the substrate. In contrast, ablation progressed to the quartz substrate when the pulse energy reached 5 nJ. Clearly, the ablation threshold of the quartz was higher than that of the PEG film, which was exploited to fabricate nanoscale features in the polymer film without incurring damage to the quartz substrate.

The size of the ablated features was dependent on laser fluence, optics, and polymer film thickness. The smallest ablated feature diameter was ~150 nm obtained using a 100x objective on a 15 nm thin film. On similar films using 50x and 10x objectives, the smallest diameters of the ablated pits were ~250 nm and ~1000 nm, respectively. Fig. 3 shows the linear relation between the squared ablated spot diameter and the logarithm of the average laser fluence for quartz and films of different thickness with 10x and 100x objective lenses. A square diameter-regression technique was used to calculate the ablation threshold and the Gaussian laser beam spot diameter [23, 24]. The method was necessary for thin film ablation studies, since the direct ablation depth measurement to determine ablation threshold [7] cannot be implemented when the ablation depth exceeds the film thickness. The $1/e^2$ laser spot radius (w_0) was calculated using the relation between the Gaussian spatial beam profile and the radial distribution of the laser fluence [23,25].

$$D^2 = 2\omega_0^2 ln\left(\frac{\varnothing_0}{\varnothing_{th}}\right) \qquad (1)$$

where D is a diameter of ablated features and f_0 is the average laser fluence that is defined as the pulse energy per unit irradiated area:

$$\varnothing_0 = \frac{E_{pulse}}{\pi\omega_0^2} \qquad (2)$$
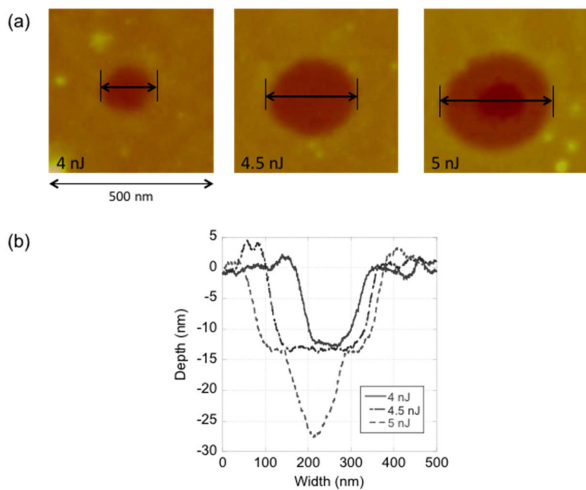

Fig. 2. Single-shot laser ablated craters using an atomic force microscope. (a) Top view AFM images of craters with three different pulse energies showing measured line for cross-section images. (b) Cross-section profiles of the ablated craters.
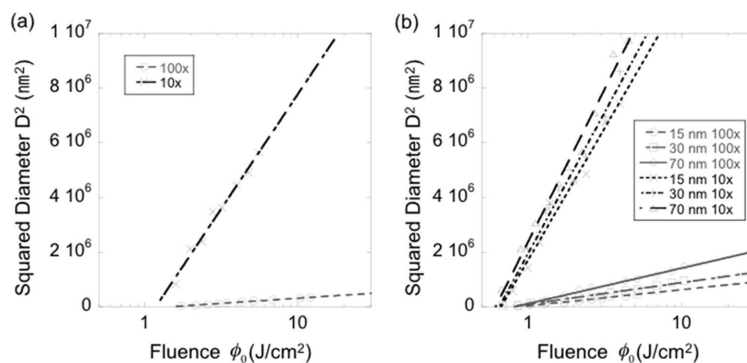

Fig. 3. The squared diameters of the ablated craters on (a) quartz and (b) three different thickness films as a function of the incident laser fluence for 10x and 100x objective lenses.

where E_{pulse} is a total pulse energy. The ablation threshold was defined as the fluence where the linear fit crosses $D^2 = 0$. The ablation thresholds for PEG films were $0.62 \sim 0.67$ J/cm^2 with 10x objective, $0.96 \sim 1.00$ J/cm^2 with 50x objective, and $0.82 \sim 0.88$ J/cm^2 with 100x objective. For the same objective lens, the ablation threshold was not affected by the film thickness.

These experimental results suggest a non-thermal ablation process. In thermal diffusion-based ablation of photosensitive polymers, the ablation threshold fluence increases dramatically with decreasing film thickness [12]. Clean ablation contours were fabricated by the femtosecond laser as shown in Fig. 2. The material damage is confined within a small region at the peak of the Gaussian laser beam distribution, where the intensity suffices to trigger multiphoton initiated avalanche ionization. Due to short pulse duration below lattice coupling time (estimated of the order of 10 ps), the heat affected zone is minimized, resulting in no lateral damage. Furthermore, the ablation threshold fluence is independent of the film thickness. The ablation thresholds for quartz are 1.18 (10x), 1.45 (50x) and 1.48 (100x) J/cm^2, respectively, and about 1.5 times higher than the respective of PEG film. Therefore, clear PEG ablated pit arrays can be fabricated without damaging the underlying quartz substrate.

Using (1), the *effective* diameter of laser beam focused on the surface can be calculated from the slope of the plot in Fig. 3, $2w_0^2$. This parameter is a derivative of the applied fitting procedure and was found to increase with increasing PEG film thickness. Consequently, the $1/e^2$ laser spot radii (w_{0q}) on quartz were used as a reference for determining the laser fluence for all cases (PEG and quartz ablation). A few groups have reported there is no effect of thin film thickness on the ablation efficiency [15,26]; however, their laser beam spot sizes were much bigger (10~20 μm beam diameters) than in the present study (0.86~4 μm beam diameters). Although the processing laser beam spot on the surface was set by the focusing optics, the ablated feature diameters were dependent on the film thickness when the beam was tightly focused. It is noted that the transient pressure generated by vigorous intramolecular interactions and vibration excited by the laser irradiation is an important mechanism of polymer thin film ablation [27,28]. In this study, the film thickness ($10 \sim 70$ nm) is thinner than the optical penetration depth of the nonlinear absorption of 100 fs laser
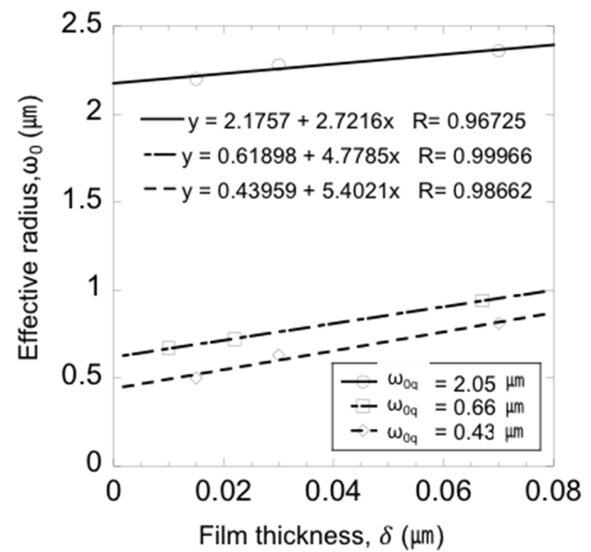

Fig. 4. Effective radius (w_0), calculated beam spot radii on PEG thin films, as a function of film thickness for three different calculated beam spot radii on the quartz (w_{0q}).
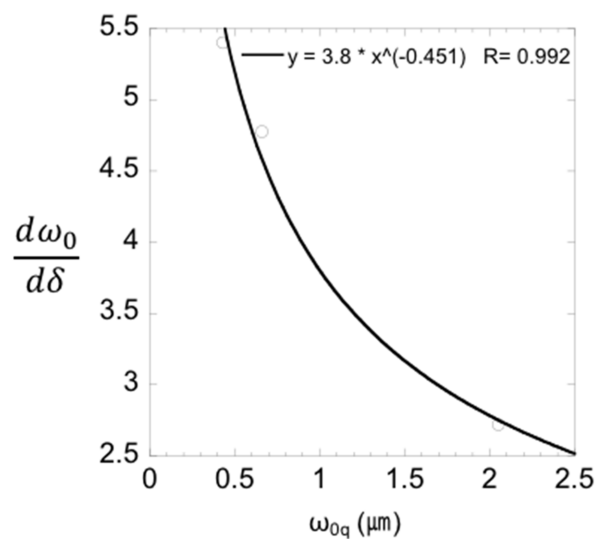

Fig. 5. Increasing rate of effective radii depending on film thickness ($dw_0/d\delta$) as a function of the calculated beam spot radii on the quartz (w_{0q}). The slope of the increase of the effective radii depending on the film thickness (δ) decreases by a $w_{0q}^{-0.45}$ dependence

pulses at 400 nm wavelength, which means electron-photon energy transition takes place through the whole thickness of the films. While the electron excitation energy relaxes, mechanical stress is accumulated in the film due to transient pressure generated by the molecular motion. The stress induces material fracture and destruction because the irradiated volume is confined by intact film and the rigid substrate [28]. Therefore, the bigger size ablation features on the thicker film were obtained because the mechanical

stress propagates longer and wider in the thicker films. Fig. 4 shows the effective radii, the calculated $1/e^2$ laser spot radii (w_0) on the thin film, depending on the film thickness and the calculated $1/e^2$ laser spot radii (w_{0q}) on the quartz. The slope of the increase of the effective radii depending on the film thickness (δ) decreases by a $w_{0q}^{-0.45}$ dependence as shown in Fig. 5. It is noted that the film thickness effect should decrease when the laser beam spot becomes bigger comparing to the dispersion length of the mechanical stress.

4. Conclusion

Femtosecond laser ablation of PEG brush layers with various thicknesses was investigated by examining the profiles of single pulse craters with AFM. The ablation threshold of the thin film was not influenced by the film thickness when the ablation occurs mainly by the nonthermal process. However, the film thickness influenced the ablated crater diameters. Larger features were fabricated in thicker films with the same laser irradiated fluence due to the mechanical stress propagation. Because of the higher ablation threshold of quartz than PEG films, clear ablation pit arrays can be fabricated without damage to the substrate. Here, fabrication of ablation craters of diameter as small as ~150-nm was achieved. Future studies will address the photochemical reaction of the polymer films irradiated by the femtosecond laser with low fluences below ablation threshold.

Acknowledgment

References

[1] D. A. Higgins, T. A. Everett, A. F. Xie, S. M. Forman, T. Ito, High-resolution direct-write multiphoton photolithography in poly (methylmethacrylate) films, Appl. Phys. Lett. 88 (2006) 184101.

[2] S. Ibrahim, D. A. Higgins, T. Ito, Direct-write multiphoton photolithography: A systematic study of the etching Behaviors in various commercial polymers, Langmuir 23 (2007) 12406-12412.

[3] Costas. P. Grigoropoulos, Transport in Laser Microfabrication: Fundamentals and Applications, Cambridge University Press, NEW YORK (2009) 398.

[4] B. N. Chichkov, C. Momma, S. Nolte, F. von Alvensleben, A. Tunnermann, Femtosecond, picosecond and nanosecond laser ablation of solids, Appl. Phys. A 63 (1996) 109-115.

[5] B. C. Stuart, M. D. Feit, A. M. Rubenchik, B. W. Shore, M. D. Perry, Laser-induced damage in dielectrics with nanosecond to subpicosecond pulses, Phys. Rev. Lett. 74 (1995) 2248-2251.

[6] F. Korte, J. Serbin, J. Koch, A. Egbert, C. Fallnich, A. Ostendorf, B. N. Chichkov, Towards nanostructuring with femtosecond laser pulses, Appl. Phys. A 77 (2003) 229-235.

[7] D. J. Hwang, C. P. Grigoropoulos, T. Y. Choi, Efficiency of silicon micromachining by femtosecond laser pulses in ambient air, J. Appl. Phys. 99 (2006) 083101.

[8] N. Hartmann, S. Franzka, J. Koch, A. Ostendorf, B. N. Chichkov, Subwavelength patterning of alkylsiloxane monolayers via nonlinear processing with single femtosecond laser pulses, Appl. Phys. Lett. 92 (2008) 223111.

[9] H. Furutani, H. Fukumura, H. Masuhara, T. Lippert, A. Yabe, Laser-induced decomposition and ablation dynamics studied by nanosecond interferometry .1. A triazenopolymer film, J. of Phys. Chem. A 101 (1997) 5742-5747.

[10] T. Lippert, Interaction of photons with polymers: From surface modification to ablation, Plasma Proc. Polym. 2 (2005) 525-546.

[11] N. Arnold, N. Bityurin, D. Bauerle, Laser-induced thermal degradation and ablation of polymers: bulk model, Appl. Surf. Sci. 138 (1999) 212-217.

[12] R. Fardel, M. Nagel, T. Lippert, F. Nuesch, A. Wokaun, B. S. Luk'yanchuk, Influence of thermal diffusion on the laser ablation of thin polymer films, Appl. Phys. A 90 (2008) 661-667.

[13] B. Lukyanchuk, N. Bityurin, S. Anisimov, A. Malyshev, N. Arnold, D. Bauerle, Photophysical ablation of organic polymers: The influence of stresses, Appl. Surf. Sci. 106 (1996) 120-125.

[14] A. Vogel, V. Venugopalan, Mechanisms of pulsed laser ablation of biological tissues, Chem. Rev. 103 (2003) 577-644.

[15] J. Bonse, J. Solis, L. Urech, T. Lippert, A. Wokaun, Femtosecond and nanosecond laser damage thresholds of doped and undoped triazenepolymer thin films, Appl. Surf. Sci. 253 (2007) 7787-7791.

[16] S. Baudach, J. Bonse, J. Kruger, W. Kautek,

Ultrashort pulse laser ablation of polycarbonate and polymethylmethacrylate, Appl. Surf. Sci. 154 (2000) 555-560.

[17] H. Kumagai, K. Midorikawa, K. Toyoda, S. Nakamura, T. Okamoto, M. Obara, Ablation of Polymer-Films by a Femtosecond High-Peak-Power Ti Sapphire Laser at 798-Nm, Appl. Phys. Lett. 65 (1994) 1850-1852.

[18] H. Jeon, R. Schmidt, J. E. Barton, D. J. Hwang, L. J. Gamble, D. G. Castner, C. P. Grigoropoulos, K. E. Healy, Chemical Patterning of Ultrathin Polymer Films by Direct-Write Multiphoton Lithography, J. Am. Chem. Soc. 133 (2011) 6138-6141.

[19] E. A. Cavalcanti-Adam, D. Aydin, V. C. Hirschfeld-Warneken, J. P. Spatz, Cell adhesion and response to synthetic nanopatterned environments by steering receptor clustering and spatial location, Hfsp Journal 2 (2008) 276-285.

[20] J. Tang, R. Peng, J. D. Ding, The regulation of stem cell differentiation by cell-cell contact on micropatterned material surfaces, Biomaterials 31 (2010) 2470-2476.

[21] Q. Cheng, S. Li, K. Komvopoulos, Plasma-assisted surface chemical patterning for single-cell culture, Biomaterials 30 (2009) 4203-4210.

[22] H. W. Ma, D. J. Li, X. Sheng, B. Zhao, A. Chilkoti, Protein-resistant polymer coatings on silicon oxide by surface-initiated atom transfer radical polymerization, Langmuir 22 (2006) 3751-3756.

[23] A. Ben-Yakar, R. L. Byer, Femtosecond laser ablation properties of borosilicate glass, J. Appl. Phys. 96 (2004) 5316-5323.

[24] N. Sanner, O. Uteza, B. Bussiere, G. Coustillier, A. Leray, T. Itina, M. Sentis, Measurement of femtosecond laser-induced damage and ablation thresholds in dielectrics, Appl. Phys. A. 94 (2009) 889-897.

[25] J. M. Liu, Simple technique for measurements of pulsed gaussian-beam spot sizes, Opt. Lett. 7 (1982) 196-198.

[26] S. Hermann, N. P. Harder, R. Brendel, D. Herzog, H. Haferkamp, Picosecond laser ablation of SiO_2 layers on silicon substrates, Appl. Phys. A. 99 (2010) 151-158.

[27] H. Masuhara, T. Asahi, Y. Hosokawa, Laser nanochemistry, Pure and Appl. Chem. 78 (2006) 2205-2226.

[28] Y. Hosokawa, M. Yashiro, T. Asahi, H. Masuhara, Photothermal conversion dynamics in femtosecond and picosecond discrete laser etching of Cu-phthalocyanine amorphous film analysed by ultrafast UV-VIS absorption spectroscopy, J. of Photochem. and Photobio. A. 142 (2001) 197-207.